vaccines

MDPI

Article

CT584 Is Not a Protective Vaccine Antigen against Respiratory Chlamydial Challenge in Mice

Steven Hoang-Phou [1], Sukumar Pal [2], Anatoli Slepenkin [2], Abisola Abisoye-Ogunniyun [1], Yuliang Zhang [1], Sean F. Gilmore [1], Megan L. Shelby [1], Feliza A. Bourguet [1], Mariam V. Mohagheghi [1], Aleksandr Noy [1], Amy Rasley [1], Luis M. de la Maza [2] and Matthew A. Coleman [1,*]

[1] Physical and Life Sciences Directorate, Lawrence Livermore National Laboratory, Livermore, CA 94551, USA; hoangphou1@llnl.gov (S.H.-P.); abisoyeogunn1@llnl.gov (A.A.-O.); zhang42@llnl.gov (Y.Z.); gilmore24@llnl.gov (S.F.G.); shelby4@llnl.gov (M.L.S.); bourguet1@llnl.gov (F.A.B.); mohagheghi1@llnl.gov (M.V.M.); noy1@llnl.gov (A.N.); rasley2@llnl.gov (A.R.)

[2] Department of Pathology and Laboratory Medicine, University of California, Irvine, CA 92697, USA; spal@uci.edu (S.P.); aslepenk@uci.edu (A.S.); lmdelama@uci.edu (L.M.d.l.M.)

* Correspondence: coleman16@llnl.gov

Abstract: Background:*Chlamydia trachomatis* is the most prevalent bacterial sexually transmitted pathogen in humans worldwide. Since chlamydial infection is largely asymptomatic with the potential for serious complications, a preventative vaccine is likely the most viable long-term answer to this public health threat. Cell-free protein synthesis (CFPS) utilizes the cellular protein manufacturing machinery decoupled from the requirement for maintaining cellular viability, offering the potential for flexible, rapid, and decentralized production of recombinant protein vaccine antigens. **Methods:** Here, we use CFPS to produce the full-length putative chlamydial type three secretion system (T3SS) needle-tip protein, CT584, for evaluation as a vaccine antigen in mouse models. High-speed atomic force microscopy (HS-AFM) (RIBM, Tsukuba, Japan) imaging and computer simulations confirm that CFPS-produced CT584 retains a native-like structure prior to immunization. Female mice were primed with CT584 adjuvanted with CpG-1826 intranasally (i.n.) or CpG-1826 + Montanide ISA 720 intramuscularly (i.m.), followed four weeks later by an i.m. boost before respiratory challenge with 10^4 inclusion forming units (IFU) of *Chlamydia muridarum*. **Results:** Immunization with CT584 generated robust antibody responses but weak cell-mediated immunity and failed to protect against i.n. challenge as demonstrated by body weight loss, increased lung weights, and the presence of high numbers of IFUs in the lungs. **Conclusion:** While CT584 was not a protective vaccine candidate, the speed and flexibility with which CFPS can be used to produce other potential chlamydial antigens make it an attractive technique for antigen production.

Keywords: *Chlamydia*; vaccine; immunization; mice; type-three secretion system; CT584; cell-free protein synthesis

Citation: Hoang-Phou, S.; Pal, S.; Slepenkin, A.; Abisoye-Ogunniyun, A.; Zhang, Y.; Gilmore, S.F.; Shelby, M.L.; Bourguet, F.A.; Mohagheghi, M.V.; Noy, A.; et al. CT584 Is Not a Protective Vaccine Antigen against Respiratory Chlamydial Challenge in Mice. *Vaccines* **2024**, *12*, 1134. https://doi.org/10.3390/vaccines12101134

Academic Editor: Victor Adekanmbi

Received: 21 June 2024
Revised: 23 September 2024
Accepted: 24 September 2024
Published: 3 October 2024

1. Introduction

Chlamydia trachomatis (*Ct*) is the most common bacterial sexually transmitted pathogen worldwide and a large public health threat [1]. Untreated infections, particularly in women, can result in serious sequelae, including pelvic inflammatory disease and infertility [2,3]. Since *Ct* infections are often asymptomatic, community surveillance is key to understanding prevalence. While the rates of infection have trended downward in the 2000s, that trend has been reversing over the last decade [4]. Alarmingly, community surveillance and testing for chlamydia seriously declined during the SARS-CoV-2 pandemic, with measured rates of infection diverging from predicted case rates, suggesting the possibility of missed diagnoses [5]. Due to the difficulties in controlling asymptomatic diseases or those with long incubation times, as exemplified by SARS-CoV-2, it is clear that a vaccine against *Ct* would be the most effective approach to limit infection spread and protect public health.

Many different chlamydial antigens have been tried in vaccine development and it remains an area of active investigation. Whole-cell fixed or attenuated chlamydial elementary bodies (EBs) offer some of the best protection from subsequent infections in mouse models [6], but ambiguity in the safety of previous human trachoma vaccine field trials [7,8] and scalability of EB production in the context of mass human vaccinations remain an important barrier. Recombinant protein antigens have seen some success in animal vaccine trials, largely focused on the major outer membrane protein (MOMP), which comprises ~60% of the mass of the chlamydial outer membrane [9]. While formulations using variations of this antigen have shown the most promise, other protein antigens present on the cell surface have been tested with varying results (reviewed in [10]).

One promising candidate is the chlamydial type III secretion system (T3SS) "injectosome" protein complex. The T3SS is responsible for the translocation of effectors from the chlamydial cytosol into the host cell cytoplasm, promoting chlamydial virulence [11]. It is comprised of over 10 different proteins, partially protruding from the chlamydial cell surface, presenting a few potential antigenic targets. Importantly, the T3SS is present at all stages of the chlamydial life cycle [12], and inhibition of the T3SS has been demonstrated to reduce chlamydial infection in cells [13–15]. Recently, a recombinant protein antigen consisting of a CopB, CopD, and CT584 fusion has been shown to confer partial protection, reducing fallopian tube pathology and bacterial load in *Chlamydia muridarum* (*Cm*) challenge studies and bacterial load in *Ct* challenge studies in mouse models [16,17]. The proteins CopB and CopD are thought to form the terminal translocon pore, while CT584 has been suggested to be the needle-tip protein of the T3SS [18–20].

CT584, as a putative needle tip protein in the chlamydial T3SS and a natural immunogen found in *Ct*-infected women [21], makes an excellent target for potential vaccine formulations. Targeting and inhibition of other needle tip proteins, such as LcrV in *Yersinia pestis*, prevents the secretion of translocon and effector proteins, precluding apoptosis of infected cells [22,23]. CT584 from *Ct* serovar D is highly conserved (97.27% identical) at the amino acid sequence level with its homolog TC0873 in *Cm* (Supplementary Figure S1). Since *Cm* infection mouse models produce similar infection and long-term sequelae to *Ct* infection in humans [24,25] and vaccine formulations containing *Ct* CT584 have shown promising results in both *Cm* and *Ct* mouse models [16,17], we hypothesized using CT584 alone as a vaccine antigen in *Cm* mouse models may induce protective adaptive immune responses that limit infection and pathology and could potentially translate well to the clinic.

Depending on the protein being tested, antigen production for immunization studies can be challenging. Cell-free protein synthesis (CFPS) offers a rapid and flexible way to express and test potential protein antigens. Coupled transcription-translation CFPS systems utilize cell lysates containing an RNA polymerase, ribosomal complexes, amino acids, nucleotides, and typically an ATP regeneration system to maintain protein synthesis, while a plasmid DNA template is added to direct mRNA synthesis and protein production [26]. *Escherichia coli*-based lysates are currently the best-characterized and highest-performing system for CFPS applications, yielding >2 mg protein per mL of reaction in less than 16 h (Reviewed in [27]). CFPS is also scalable, offering the ability to rapidly switch gears and produce other proteins—only the DNA template needs to be changed. CFPS methods are gaining popularity due to their ease of use, scalability, and rapid production, and the first CFPS-produced therapeutics [28,29] and vaccines [30] are entering clinical trials.

Here, we applied *E. coli*-based CFPS to rapidly produce and then characterize recombinant CT584 protein based on the *Ct* serovar D amino acid sequence as a potential vaccine antigen. We produced >1 mg of pure, native-like protein per mL CFPS reaction for use in immunization and testing in mouse models of chlamydial infection. We show that robust IgG antibody responses to CT584 immunization are generated using different routes of immunization and antigen/adjuvant formulations; however, the formulations of CT584 we tested were ultimately not protective against respiratory *Cm* challenges. Furthermore, we did not detect CT584 protein in chlamydial EB using EB immune sera, while CT584

immune sera could detect it, suggesting that CT584 is not as immunodominant as other *Cm* EB proteins in mouse protection experiments.

2. Materials and Methods

2.1. Plasmids and Sequences

The amino acid sequence from *Ct* CT584 (PDB: 4MLK_A) was reverse-translated, codon optimized for expression in *E. coli* and synthesized by Genscript with a short linker (AAALE) sequence before a C-terminal 6x histidine affinity purification tag. The gene fragment was cloned into the NdeI-BamHI sites in pIVEX2.3d for T7 polymerase-based expression. Amino acid sequences from *Cm* TC0873 and *Ct* CT584 were downloaded from Uniprot using accession ID's Q9PJF6 and O84588, respectively. *Cm tc0873* and *Ct ct584* gene sequences were downloaded from NCBI through ChlamBase [31] using accession ID's NC_002620.2 (locus: 1010962.1011513, + strand) and NC_000117.1 (locus 657866.658417, + strand), respectively. Sequence homology was compared using the Smith-Waterman algorithm in SnapGene, software version 7.2.

2.2. Stocks of C. muridarum

Cm (strain Nigg II; American Type Culture Collection) was grown in HeLa-229 cells using high glucose Dulbecco's medium, plus cycloheximide (1 μg/mL) and gentamycin 10 μg/mL, without fetal bovine serum. Elementary bodies (EB) were purified and stored in sugar phosphate glutamate buffer (SPG) at −80 °C as described [9]. The number of *Cm* inclusion forming units (IFU) in the stock was assessed in HeLa-229 cells using immune-peroxidase staining with a *Cm*-MOMP specific mAb (MoPn-40) produced in our laboratory [32].

2.3. Cell-Free Protein Synthesis of CT584 and Purification Strategies

CT584 protein was produced using cell-free protein synthesis kits in a continuous-exchange cell-free (CECF) device (Biotech Rabbit, Berlin, Germany, #BR1400201) according to manufacturer protocols at 1 mL scale. Briefly, lyophilized *E. coli* lysate, reaction buffer, amino acids, and feed buffer were resuspended using the supplied reconstitution buffer supplemented with an EDTA-free protease inhibitor tablet (Roche, Basel, Switzerland, #5892791001). The individual components were combined, and CT584-His in pIVEX2.3d plasmid was added to the reaction mixture at 15 μg/mL.

Small-scale reactions (25 μL) were performed by incubating the reaction mixture at 800 rpm and 30 °C overnight in a ThermoMixer C (Eppendorf, Hamburg, Germany). BODIPY labeled tRNA-Lys (Promega, Madison, WI, USA, #L5001) was included in the reaction at 1:200 *v*/*v* to track protein production. CT584 protein in total CFPS reactions was assessed by SDS-PAGE using fluorescence readings from BODIPY tRNA-Lys incorporation and SYPRO Ruby (ThermoFisher, Waltham, MA, USA, #S12000) total protein stains. Larger-scale reactions (1 mL) to produce protein for vaccine studies utilized the CECF device from the kit manufacturer. The reaction was incubated at 30 °C for 16 h while shaking at 300 rpm in a bacterial floor shaker.

After incubation of large-scale reactions, the CFPS reaction mixture was removed from the CECF device and purified using Ni^{+2}-Nitrilotriacetic acid (NTA) affinity chromatography. 500 μL of Ni^{+2}-NTA beads (Roche, Basel, Switzerland, #5893682001) were loaded onto a 12 mL column and equilibrated into six packed bead volumes of equilibration buffer (50 mM Tris, 300 mM NaCl, and 10 mM imidazole, pH 8.0). The CFPS reaction mixture was applied to the column and allowed to incubate at 4 °C for 1 h while mixing on a nutator. Afterward, the column was washed with 12 packed bead volumes of wash buffer (50 mM Tris, 300 mM NaCl, and 20 mM imidazole, pH 8.0). CT584 was eluted in 300 μL fractions, first with 1.8 mL of elution buffer (50 mM Tris, 300 mM NaCl, and 250 mM imidazole, pH 8.0) and then 300 μL of elution buffer containing 500 mM imidazole.

Elution fractions 2–7 were pooled and concentrated to 200 μL using a 10k MWCO Amicon filtration column (MilliporeSigma, Burlington, MA, USA, #UFC501096). The

concentrated protein was injected into a Superdex 200 Increase 10/300 GL (GE Healthcare, Chicago, IL, USA, #28-9909-44) size exclusion column chromatography system (Waters, Milford, MA, USA) to further purify the protein. Peak fractions were collected and pooled for further downstream analysis.

2.4. Purification of C. muridarum recombinant MOMP (rMOMP)

Cm MOMP was produced in *E. coli* and extracted from inclusion bodies as described previously [33]. Briefly, *E. coli* BL21 (DE3) cells were transformed with the plasmid containing *C. muridarum* MOMP DNA and inoculated into LB broth. rMOMP was extracted from *E. coli* inclusion bodies and purified using a Sephacryl-S-300 column (Sigma-Aldrich, St. Louis, MO, USA) column (1 × 50 cm) which was pre-equilibrated with 100 mM Tris–HCl, pH 8.0, 200 mM NaCl, 10 mM EDTA, 0.02 mM DTT, and 0.05% Z3-14 and the peak fractions containing rMOMP were pooled. Before immunization, recombinant protein was dialyzed against PBS (pH 7.4) with 0.05% Z3-14. By the Limulus amoebocyte assay (Associates of Cape Cod Inc.; East Falmouth, MA, USA), rMOMP preparations had less than 0.05 EU of LPS/mg of protein.

2.5. HS-AFM Data Collection

HS-AFM images of protein complexes were acquired in tapping mode at room temperature using an HS-AFM instrument (RIBM, Tsukuba, Japan) equipped with ultra-short AFM cantilevers (Nanoworld, Neuchatel, Switzerland, USC-F1.2-k0.15-10) with EBD tip (radius < 5 nm). This instrument utilizes a dynamic proportional-integral-differential (PID) controller [34,35] to eliminate probe "parachuting" artifacts from images and reduce the tip-sampling forces. The HS-AFM fluid cell was filled with 120 µL buffer solution (20 mM HEPES (pH 7.2), 150 mM KCl, 1 mM DTT, 1 mM EDTA, 1 mM EGTA), and constant volume was maintained with a custom-built perfusion system. In a typical experiment, we collected 128 pixel × 128 pixel images from a 50 nm × 50 nm area at a scan rate of 3 frames per second.

2.6. HS-AFM Data Processing and Analysis

Raw HS-AFM image data were converted to ImageJ (developed by Wayne Rasband, National Institutes of Health, Bethesda, MD, USA) stacks using custom software developed in (10.1098/rstb.2016.0226) [36]. The line plots were generated by a custom IgorPro 8 software (WaveMetrics, Lake Oswego, OR, USA). The simulated AFM images were generated by using open-source code [37]. The volume of protein oligomer from experimental data and simulated AFM images was calculated by using Gwyddion software version 2.63 [38].

2.7. Vaccination of Female BALB/c Mice

For challenge studies, four-to-five-week-old female BALB/c (H-2d) mice (n = 5 mice per group, Charles River Laboratories, Wilmington, MA, USA) were obtained and housed in the University of California, Irvine, vivarium and experiments carried out according to the approved Institutional Animal Care and Use Committee (IACUC) protocol. Mice were vaccinated with CT584 (20 µg/mouse/immunization), rMOMP (20 µg/mouse/immunization), or PBS using two different regimens: (1) Intranasal (i.n.) prime and intramuscular (i.m.) boost in the quadriceps muscle at a four-week interval; and (2) i.m. prime and boost four weeks apart in the quadriceps muscle. CT584 + rMOMP (10 µg/mouse/immunization of each antigen) was also tested in the i.n./i.m. vaccination regime. *Cm* EBs (10^4 IFUs) were given in a single i.n. dose at the time of the first immunization as a positive control. The following adjuvant combinations were used for all groups: CpG-1826 (Tri-Link, San Diego, CA, USA) (10 µg/mouse/immunization) + Montanide ISA 720 VG (Seppic Inc., Fairfield, NJ, USA) [32] at 70% (v/v) of the final dose. For i.n. immunizations, only CpG-1826 (10 µg/mouse/immunization) was used. For all i.m. vaccinations, Montanide ISA 720 VG was mixed with CT584 and CpG-1826 using a vortex (Fisher Scientific, Waltham, MA, USA). The formulation was vortexed for one minute, followed by one minute rest on ice. The cycle was repeated five times.

For alternative adjuvant studies, 5-week-old female BALB/c (H-2d) mice were obtained and housed in the Lawrence Livermore National Laboratory vivarium, and experiments were carried out according to the approved IACUC protocol. Mice were vaccinated i.m. with CT584 (10 μg/mouse/immunization) adjuvanted with CAF01 (50 μg) + R848 (Invivogen, San Diego, CA, USA) (20 μg) or PBS alone (unadjuvanted) in a three-week interval prime-boost-boost regime. CAF01 is a liposomal adjuvant [39] prepared by mixing dimethyldioctadecylammonium (DDA) bromide (Avanti, Alabaster, AL, USA) and a,a′-trehalose 6,6′-dibehenate (TDB) (Avanti). Briefly, DDA is mixed with TDB in a 5:1 μg ratio, dried under a nitrogen stream with continuous agitation, and desiccated in a vacuum overnight before resuspension in water. After resuspension, the liposomes are heated at 57 °C for 20 min while shaking and then sonicated for 10 min before addition to the antigen.

2.8. Intranasal Challenge with Cm EBs and Evaluation of the Course of the Infection in Mice

Anesthetized mice were challenged i.n. with 10^4 IFU of *Cm* four weeks after the second immunization [40]. Daily body weight changes were assessed for 10 days post-challenge (d.p.c.), after which the mice were euthanized, and their lungs were weighed and homogenized (Seward Stomacher 80; Lab System, Fairham, Nottingham, UK) in 5 mL of SPG. To establish the number of *Cm* IFUs, six serial dilutions of the lungs' homogenates were used to infect Hela-229 cells grown in 48 well plates. Following incubation for 30 h at 37 °C in a CO_2 incubator, the IFU were visualized with mAb MoPn-40, and counted using a light microscope [41]. The limit of detection (LD) was <50 *Cm* IFU/lungs/mouse.

2.9. Antibody Titer Determination

Blood from the periorbital plexus was collected the day before the respiratory challenge. Antibody titers to *C. muridarum* EBs (1 μg/well) were determined by ELISA using 96-well plates (Corning, Durham, NC, USA) as previously described [42]. Serial dilutions of serum were added, and the antigen–antibody reactions were detected with HRP-conjugated goat anti-mouse. Goat anti-mouse IgG, IgG1, and IgG2a (BD Bioscience, San Diego, CA, USA) diluted 1:5000 for IgG and 1:1000 for the two isotypes were used. ABTS [2,2′-azinobis-(3-ethylbenzthiazoline-6-sulfonate)] (Sigma-Aldrich, St. Louis, MO, USA) was utilized as the substrate and the plates were scanned in an ELISA reader at 405 nm (Labsystem Multiscan; Helsinki, Finland). Titers were calculated using the OD of pre-immunization sera ± 2 SD as a background and reported as geometric mean titer (GMT).

To evaluate the humoral immune responses to *C. muridarum* EBs in the genital mucosa, vaginal samples were collected by washing twice with 20 μL/mouse using sterile PBS before pooling for each group the day before i.n. challenge. Levels of IgG and IgA (ICN Pharmaceuticals, Costa Mesa, CA, USA; diluted 1:3500) were determined as discussed above.

CT584-specific antibody titers were quantified by ELISA as previously described [42]. Briefly, sera from PBS immunized mice were used as negative control. Ninety-six-well, high-binding plates (Corning™ 3690, Durham, NC, USA) were coated with 100 μL of CT584 at a concentration of 10 μg of protein/mL and incubated overnight at 4 °C. Serum was added to each well in 3-fold serial dilutions after washing and blocking for nonspecific binding. After overnight incubation, the plates were washed and incubated with one of the following secondary antibodies: Horseradish peroxidase-conjugated (HRP) goat anti-mouse IgG antibodies (KPL, Gaithersburg, MD, USA, #5220-0460), HRP rat anti-mouse IgG1 (BD Biosciences, Franklin Lakes, NJ, USA, #559626), and HRP rat anti-mouse IgG2a conjugate (BD Biosciences 553391). The binding was measured using a BioTek (Agilent, Santa Clara, CA, USA) plate reader at an optical density (OD) of 405 nm, and IgG titers were calculated using non-linear regression curve fit values.

2.10. Tissue Harvest and Single-Cell Isolation

For alternative adjuvant studies, mouse sera were collected 3 weeks after the last boost by cardiac puncture. Spleens and popliteal draining lymph nodes were also harvested. Single cells from spleens and draining lymph nodes were isolated by gently crushing

the tissues individually through a sterile 70 µm cell strainer while passing sterile HBSS (Gibco™, Grand Island, NY, USA, #14025092) supplemented with 2% heat-inactivated FBS (Gibco™ #A5669801) to wash down the cells. Following centrifugation at 1500 rpm for 5 min at 4 °C, red blood cells from the splenocytes and draining lymph node cells were lysed by resuspending the cell pellets with 3 mL of ammonium-chloride-potassium (ACK) lysing buffer (Gibco™ #A1049201) and incubation for 5 min at room temperature, followed by dilution of the mixture with 27 mL of the wash buffer (HBSS + 2% FBS) to stop the reaction. After lysis, cells were pelleted and resuspended with culture media (RPMI 1640 medium (Gibco™ #11875093) supplemented with 10% FBS) for ex vivo restimulation.

2.11. SDS-PAGE/WBs

Aliquots of total cell-free reaction or purified CT584 SEC fractions were diluted into 4x NuPAGE LDS Sample Buffer (ThermoFisher #NP0007) and 10x NuPAGE Sample Reducing Agent (ThermoFisher #NP0009) before heat denaturing. Samples were loaded onto 4–12% NuPAGE Bis-Tris gradient gels (ThermoFisher #NP0323BOX) and run at 200 V for 35 min. Gels were stained with SYPRO-Ruby Protein Gel Stain (ThermoFisher #S12000) or Coomassie Brilliant Blue R-250 (Genscript, Piscataway, NJ, USA) according to manufacturer directions and imaged on an Odyssey Fc Imager (Li-Cor) or iPhone camera on a lightbox.

Western blot was performed to detect CT584-specific antibody binding. Briefly, either the recombinant CT584 or purified *Cm* EB's were solubilized in SDS sample buffer (Novex, Life Technologies, Carlsbad, CA, USA) in the presence of reducing agent (10 mM DTT), heated in a water bath at 95–100 °C for 5 min and run on 10% SDS-PAGE gels. 1.8 µg of CT584 and 3 µg of EB lysate were loaded in their respective lanes. After electrophoresis, the resolved protein bands were transferred onto nitrocellulose membranes. The membranes were blotted with pooled mouse sera, collected as described above the day before the *Cm* challenge and diluted 1:200 in PBS as the primary antibody. The resulting antibody binding was probed with HRP goat anti-mouse immunoglobulins (IgG, IgA, IgM) (Cappel, MP Biomedicals, Santa Ana, CA, USA) as the secondary antibody and visualized with chloronaphtol substrate.

2.12. Ex Vivo Restimulation

Splenocytes and lymph node cells were seeded in 24 well plates at 1 million cells/well/sample and cultured with CT584 at a concentration of 10 µg of protein/mL or 2 µL of 500x PMA/Ionomycin cocktail (BioLegend, San Diego, CA, USA, #423301) per mL of culture media After 4 h of incubation, 1x monensin was added to enhance intracellular cytokine staining signals by blocking transport processes during cell activation.

2.13. Flow Cytometric Analysis

A 10-color T cell panel was used for flow cytometry to delineate IFN-γ and TNFα expressing CD4+ and CD8+ T cells and to evaluate changes in both CD4 and CD8 T cell subsets. Briefly, cultured splenocytes and lymph node cells were washed and resuspended in FACS staining buffer (BioLegend #420201) containing 1 µg of purified Rat Anti-Mouse CD16/CD32 (Mouse BD Fc Block) (BD Pharmingen, San Diego, CA, USA, #553141) and were kept on ice throughout staining. Cell surface staining antibodies for CD3, CD4, CD8, and also propidium iodide dye (BioLegend: #100334, #100451, #563332, and #421301, respectively) were added, and cells incubated on ice for 45 min. Cells were washed and then fixed and permeabilized using the True-Nuclear™ Transcription Factor Buffer Set (BioLegend #424401). Intracellular staining antibodies (IFN-γ (BioLegend #505810) and TNFα (BioLegend #506322)) were added as recommended in the permeabilization buffer. Following incubation, cells were washed and resuspended in FACS staining buffer for analysis on a BD FACS Celesta Cell Analyzer (BD Biosciences, San Jose, CA, USA). Flow cytometry data were analyzed using FlowJo v10 (BD Biosciences, San Jose, CA, USA).

2.14. Statistical Analyses

The Student's *t*-test was employed to evaluate differences between changes in body weight at day 10 post-challenge, lung weights, and CD4 and CD8 T cell populations. Two-way repeated measures ANOVA with Sidak's multiple comparison test was employed to compare changes in mean body weight over the 10 days of observation following the *Cm* i.n. challenge. The Mann–Whitney U Test was used to compare the number of *Cm* IFU in the lungs. Welch's *t*-test was used to compare antibody titers and data were reported as geometric mean or non-linear regression curve fit. ANOVA using Dunnett's multiple comparisons test was used to compare IFN-γ and TNF-α levels. A p-value of <0.05 was considered to be significant. A p-value of <0.1 was regarded as approaching significance.

3. Results

3.1. High Yields of CT584 Can Be Produced Using Cell-Free Protein Synthesis

Optimal production of poly-histidine tagged *Ct* CT584 (hereafter CT584) through CFPS requires a highly productive cell-free lysate, reaction buffer, and energy regeneration solution, and a plasmid containing the codon-optimized *ct584* DNA template (Figure 1A). Codon optimization introduces silent mutations into the DNA coding sequence of the template to better match tRNA frequencies and translation speeds encountered in the host cell (*E. coli*) lysate to improve translation efficiency [43]. Codon optimization of the *Ct* serovar D derived *ct584* sequence resulted in the replacement of 25.14% of its DNA bases (Figure 1B, Supplementary Figure S2). Nascent CT584 protein can be labeled through the inclusion of a BODIPY dye-labeled tRNA-Lys in the cell-free reaction, which incorporates labeled lysine residues into actively made proteins. Specific production and high yields of CT584 can be seen through BODIPY fluorescence and SYPRO Ruby staining for total protein on SDS-PAGE gels (Figure 1C).

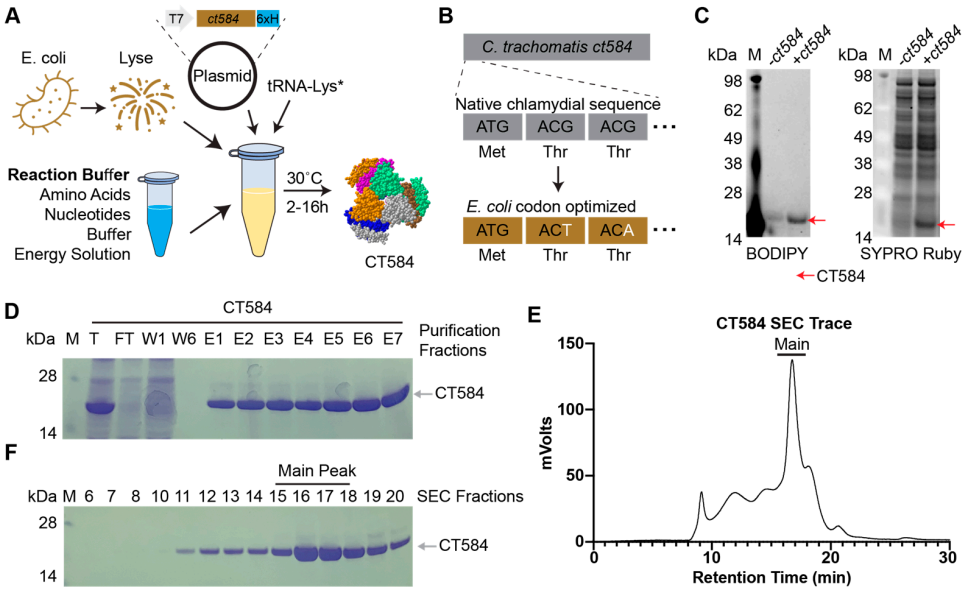

Figure 1. CT584 can be produced and purified using cell-free protein synthesis. (**A**) Schematic of the cell-free protein synthesis (CFPS) approach to protein production. (**B**) Schematic of DNA codon optimization performed on chlamydial *ct584*. (**C**) SDS-PAGE gel depicting a fluorescent image of BODIPY labeled tRNA-Lys incorporation into CT584 (left) and SYPRO Ruby total protein stain (right). (**D**) Coomassie blue stained SDS-PAGE gel showing typical affinity purification fractions for CT584. M: Marker, T: Total, FT: Flow-through, W: Wash, E: Elutions. (**E**) Smoothed histogram of size exclusion chromatography (SEC) retention times for affinity-purified CT584. (**F**) Coomassie blue stained SDS-PAGE gel of SEC elution fractions. Fractions pooled and used for further experiments are indicated ("Main Peak").

To remove impurities from the CFPS lysates, we purified CT584 using a combination of affinity chromatography and size exclusion chromatography (SEC). His-tag and Ni^{+2}-NTA affinity chromatography enriched CT584 away from other cell-free lysate proteins (Figure 1D); however, commonly seen His-tag purification contaminants from *E. coli* lysates [44] could potentially pose issues for further immunization studies and confound results. To further enrich and purify CT584, we concentrated it and performed SEC on the sample, leading to >99% pure protein, giving a final purified yield of 1.46 mg from a 1 mL CFPS reaction (Figure 1E,F).

3.2. High-Speed Atomic Force Microscopy Reveals CFPS Produced CT584 Has a Native-like Conformation

CT584 has been shown to exist in a hexameric structure [45], and since CFPS reactions typically do not include many of the native chaperones and other protein folding machinery present in the original host cell, whether CFPS-made CT584 retains that structure was an open question. Our attempts to generate full-length CT584 protein crystals for structural studies were unsuccessful. However, to confirm that our cell-free produced CT584 resembled the crystallized truncated CT584 structure, we performed high-speed atomic force microscopy (HS-AFM) to visualize its geometry and gross structure. Purified CT584 was adsorbed onto a mica surface and imaged in buffer solution using an AFM tip with a nominal probe size of 5 nm. We were able to observe individual protein units bound to the mica surface, which formed a globular shape with some sub-structure consistently visible in the AFM images. When we used the AFM images to estimate the protein volume, we obtained a value of 563.6 ± 123.6 nm^3 (Figure 2A).

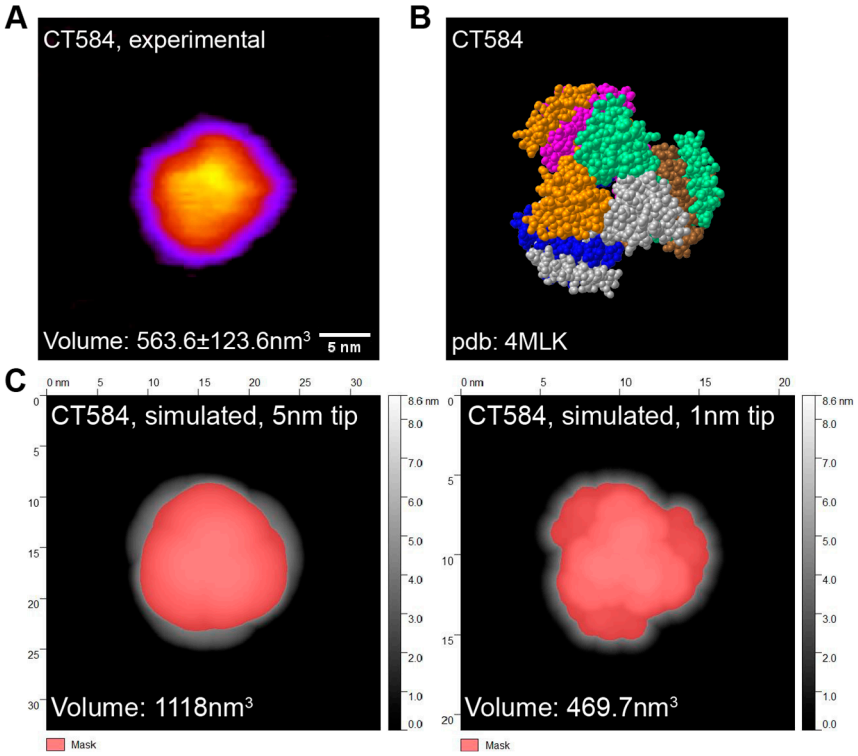

Figure 2. CFPS-produced CT584 retains a native-like conformation. (**A**) Atomic force microscopy (AFM) image of CT584. Color scale: 0.8 nm (purple) to 4.24 nm (yellow) Scale bar: 5 nm. (**B**) Space-filling model of published CT584 crystal structure (PDB: 4MLK). (**C**) Simulated AFM images using the CT584 crystal structure and a 5 nm (**left**) and 1 nm (**right**) probe size. Highlighted pink areas show coverage.

From the known crystal structure of truncated CT584 [45] (PDB: 4MLK, Figure 2B), we calculated the hypothetical volume of a CT584 hexamer from simulations using different

AFM tip sizes as a model parameter (Figure 2C). Using a nominal AFM tip size of 5 nm produced a poor fit (volume estimate of 1118 nm^3) for several reasons. First, the simulated AFM image assumed a perfectly rigid protein that does not deform like a physical sample would. Second, because of the small physical dimensions of the protein, it is likely imaged with individual asperities on the tip surface that can be significantly sharper than the nominal AFM tip size, leading to overestimates of volume. Increasing the resolution by simulating a 1 nm tip size produced a good fit with the volume estimated at 469.7 nm^3, which was close to our experimentally measured protein volume, suggesting that cell-free produced full-length CT584 may indeed exist in a similar multimeric conformation to the truncated CT584 crystal structure.

3.3. CT584 Is Immunogenic in Mouse Models and Generates an IgG Antibody Response

As a putative needle-tip protein of the T3SS, we hypothesized that CT584 could act as a suitable antigen for immunization against chlamydial infection. Both mucosal and systemic routes of immunization have been reported for recombinant protein antigens against chlamydia [46], and a priori, it is difficult to know which route will perform better. To investigate the utility of CT584 as a vaccine antigen and determine the effect of the delivery route, we designed two separate but related experiments. We injected 20 μg of CT584 or PBS adjuvanted with CpG-1826 and Montanide ISA 720 in a 28-day interval prime (i.n. or i.m.) and i.m. boost, followed by an i.n. challenge regime using female BALB/c mice (Figure 3A). rMOMP + CT584 (10 μg each) was included to examine potential combinatorial effects, and rMOMP alone and live *Cm* EBs were included as positive controls in the i.n./i.m. experiment. Due to the incompatibility of Montanide for intranasal application, the i.n. prime was only adjuvanted with CpG-1826. CpG-1826 has been reported to promote a Th1 response, while Montanide ISA 720 induces a mixed Th1/Th2 response [47,48]. Importantly, the combination has been shown to be effective as an adjuvant for chlamydial vaccines [49].

Serum and mucosal anti-EB titers were determined by ELISA, using sera and vaginal washes collected the day before the *Cm* challenge (Table 1). In both i.n. and i.m. regimes, CT584 immunized mice generated an IgG response greater than PBS immunized groups, although the response was weaker compared to rMOMP or EB immunized groups. Antibody titers from CT584 i.n./i.m. immunized mice showed a skew towards increased IgG2a compared to IgG1, indicating a more Th1-biased immune response, while CT584 i.m./i.m. immunized mice generated a more balanced Th1/Th2 immune response. Mucosal IgG and IgA antibody titers from vaginal washes were low or negligible.

Table 1. Anti-*Cm* EB antibody titers from immunized mice.

i.n./i.m. Immunization Group (*n* = 5 mice/group)	**Pooled Anti-EB Serum Dilution Titer**			**Pooled Vaginal Wash Anti-EB Titer**	
	IgG1	**IgG2a**	**IgG2a/IgG1**	**IgG**	**IgA**
CT584	800	3200	4	160	<10
Cm rMOMP	51,200	51,200	1	640	80
CT584 + *Cm* rMOMP	25,600	51,200	2	160	80
Live *Cm* EB (i.n)	1600	25,600	16	640	1280
PBS	<100	<100	-	<10	<10
i.m./i.m. Immunization group (*n* = 5 mice/group)	Anti-EB Serum Dilution Geometric Mean Titer			Pooled Vaginal Wash Anti-EB Titer	
	IgG1 (min–max)	IgG2a (min–max)	IgG2a/IgG1	IgG	IgA
CT584	3676 (1600–6400)	3200 (200–25,600)	0.9	80	<10
Cm rMOMP	38,802 (6400–204,800)	178,289 (102,400–409,600)	4.6	1280	20
PBS	<100	<100	-	<10	<10

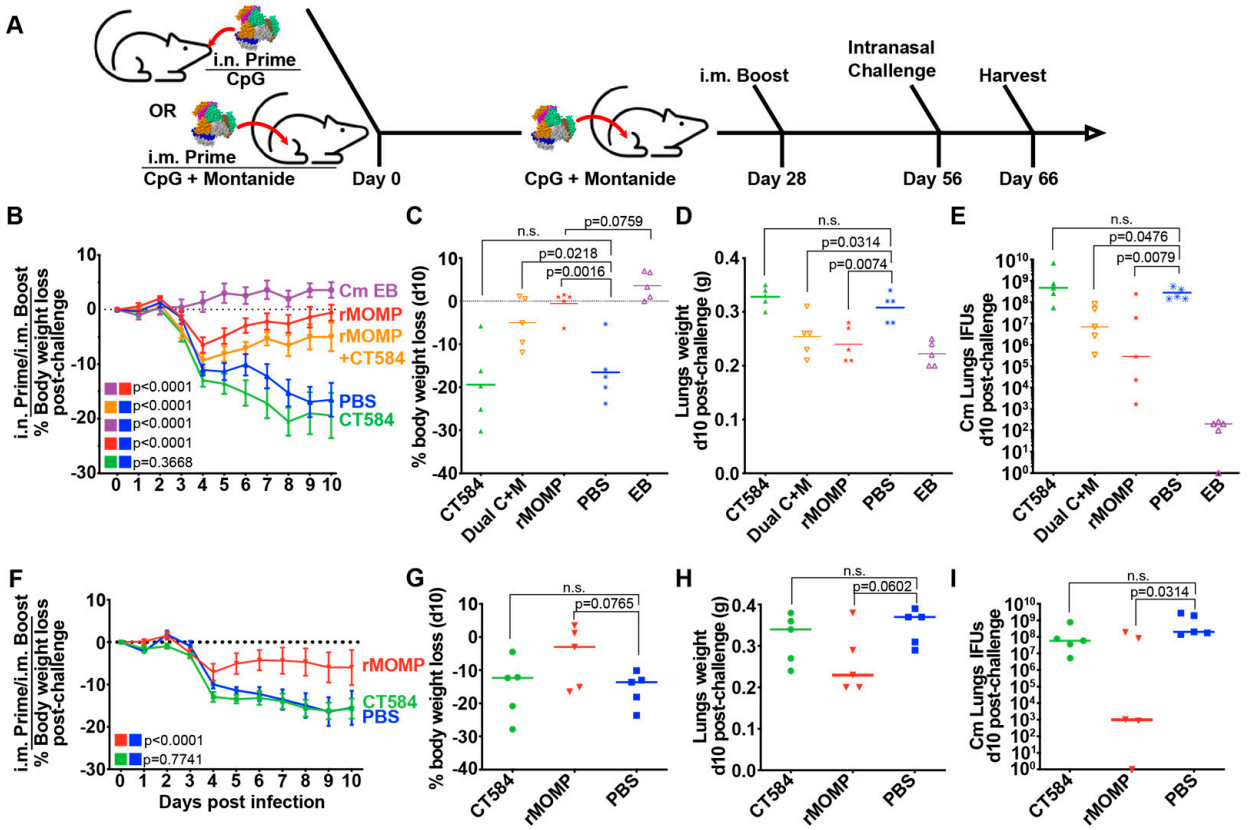

Figure 3. CT584 immunization fails to generate a protective response against an i.n. chlamydial challenge in mice. (**A**) Schematic of immunization routes and schedule for challenge studies. (**B**) Line graph depicting mean mouse weights ± s.e.m. after intranasal challenge in i.n./i.m. immunized mice. *p*-values calculated using two-way repeated measures ANOVA. (**C**) Scatter plot showing percent body weight loss at day 10 post-challenge in i.n./i.m. immunized mice. The C + M group indicates a combination vaccine using CT584 and rMOMP. The line indicates the median. *p*-values calculated using Student's *t*-test. (**D**) Scatter plot showing lung weights at day 10 post-challenge in i.n./i.m. immunized mice. The C + M group indicates a combination of CT584 and rMOMP. The line indicates the median. *p*-values calculated using Student's *t*-test. (**E**) Scatter plot showing the number of *Cm* IFUs in mouse lungs at day 10 post-challenge in i.n./i.m. immunized mice. The C + M group indicates a combination of CT584 and rMOMP. The line indicates the median. *p*-values calculated using the Mann–Whitney U test. (**F**) Line graph depicting mean mouse weights ± s.e.m. after intranasal challenge in i.m./i.m. immunized mice. *p*-values calculated using two-way repeated measures ANOVA. (**G**) Scatter plot showing percent body weight loss at day 10 post-challenge in i.m./i.m. immunized mice. The line indicates the median. *p*-values calculated using Student's *t*-test. (**H**) Scatter plot showing lung weights at day 10 post-challenge in i.m./i.m. immunized mice. The line indicates the median. *p*-values calculated using Student's *t*-test. (**I**) Scatter plot showing the number of *Cm* IFUs in mouse lungs at day 10 post-challenge in i.m./i.m. immunized mice. The line indicates the median. *p*-values calculated using the Mann–Whitney U test. $n = 5$ mice per group for all groups. n.s. = not significant.

3.4. CT584 Immunization Is Not Protective against an Intranasal C. muridarum Challenge

To test whether the immune response generated with CT584 is protective, immunized mice were challenged intranasally with 1×10^4 IFU of *Cm* four weeks after boost (Figure 3A). Mice body weights were tracked for ten days post-challenge before euthanasia, examination of lungs' weights, and determination of the number of *Cm* IFUs.

EB, rMOMP, and rMOMP + CT584 immunized groups exhibited significant differences to the PBS control group, showing lower body weight loss (Figure 3B,C,F,G), lower lung weights (Figure 3D,H), and lower IFUs recovered from the lungs (Figure 3E,I). Although

both rMOMP immunized groups showed an initial rapid weight loss from days 2–4 after challenge, they recovered to near initial body weights by day 10. In contrast, the mice immunized with CT584 alone performed similarly to the PBS negative control group, showing rapid body weight loss, increased lung weights, and higher lung IFUs recovered compared to the EB and rMOMP positive control groups.

To determine whether the CT584-induced antibodies were antigen-specific, we used pooled immune sera collected from mice one day before challenge as the primary antibody in a western blot of purified CT584 protein (Figure 4, left). As expected, the CT584 immune sera detected a single robust band at the correct molecular weight, while the PBS immune sera did not detect any protein. Unexpectedly, sera from mice immunized with *Cm* EBs also failed to detect CT584. Running the converse experiment, we blotted whole *Cm* EB lysates onto membranes and probed with the same pooled immune sera (Figure 4, right). Although CT584 immune sera could detect CT584 in EB lysates, EB immune sera could not, raising the question of whether CT584 antigens are accessible or immunogenic in EBs for antibody generation or are present in too low quantities.

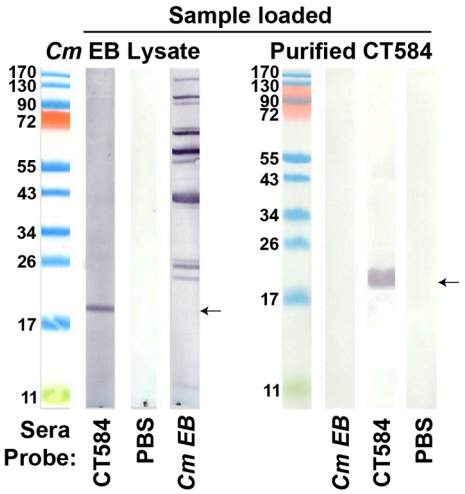

Figure 4. CT584 immune sera detect the recombinant and native protein, but *Cm* EB immune sera do not. (**Left**): Western blots of *Cm* EB lysates probed with the pooled sera of mice immunized with Lane 1—recombinant CT584; Lane 2—PBS; Lane 3—live i.n. *Cm* EB: The black arrow indicates the CT584 band. (**Right**): Western blots of purified recombinant CT584 probed with the pooled sera of mice immunized with Lane 1—i.n. *Cm* EB; Lane 2—recombinant CT584; Lane 3—PBS. The black arrow indicates the CT584 band.

Since adjuvant choice in formulations can have a significant influence on vaccine effectiveness and outcomes, we also investigated the immune response generated towards CT584 using CAF01 and R848 adjuvants in a 21-day interval i.m. prime-boost-boost regimen in BALB/C mice (Figure 5A). These adjuvants have been described to stimulate Th1/Th2 balanced and Th2-biased, respectively, immune responses [50,51]. Consistent with our previous results, we observed an IgG response induced by CT584 immunization. Furthermore, we observed elevated IgG1 vs. IgG2a antibody levels, suggesting a Th2-favored response (Figure 5B,C). To determine what T cell immune responses were induced, we examined the CD4 and CD8 T cell populations through flow cytometry after gating for single live $CD3^+$ cells (Figure 5D,E, Supplemental Figure S3A) extracted from the ex vivo restimulated draining lymph node cells and splenocytes of immunized mice. Using the extracted cells, we also performed ex vivo antigen restimulation assays. We gated for live cells in the splenocyte and lymph node cultures (Supplemental Figure S3B) and assessed markers such as IFN-γ (Figure 5F,G, left) and TNF-α (Figure 5F,G, right); however, there were no significant differences between CT584 immunized mice and PBS controls for any marker.

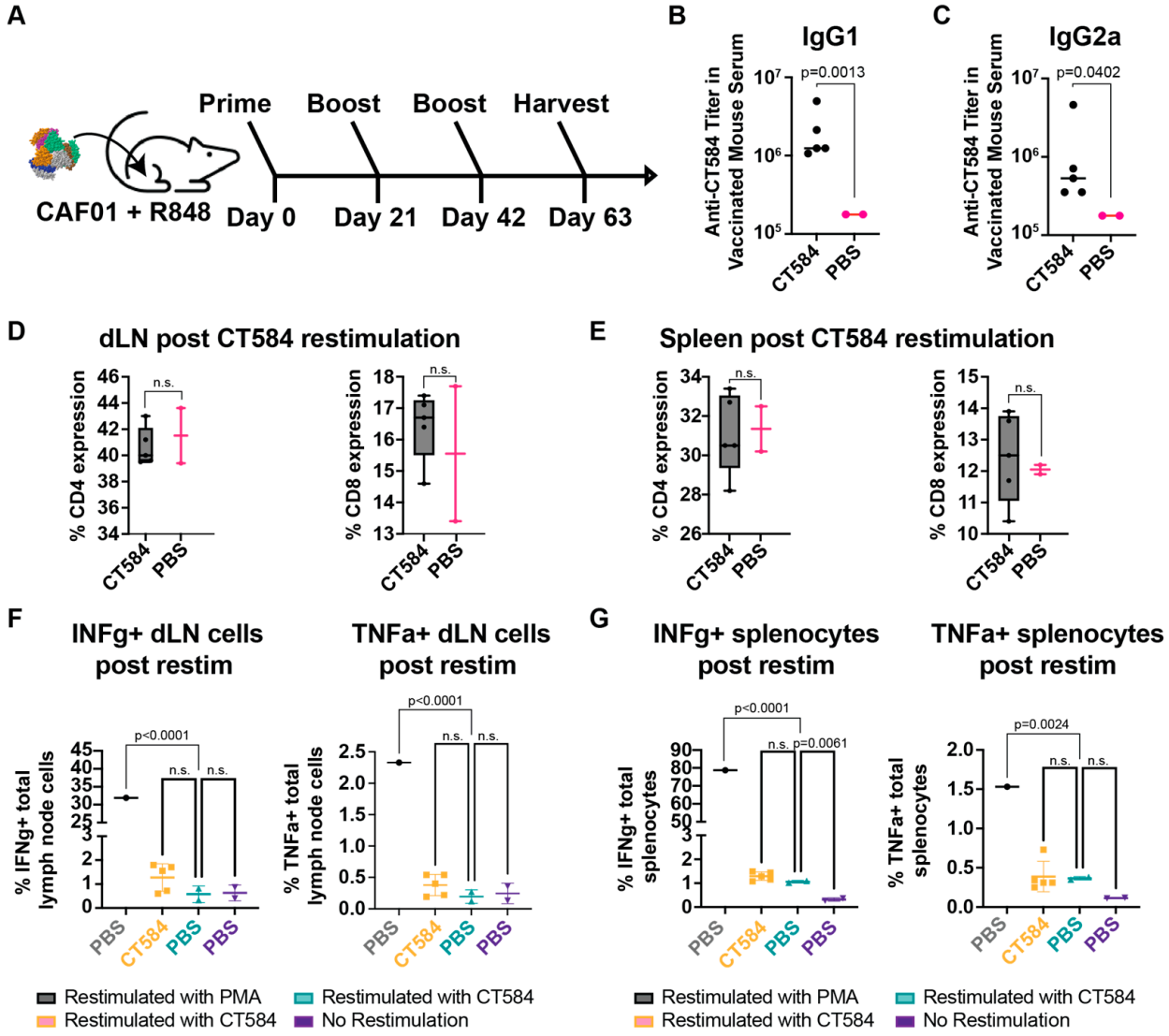

Figure 5. CT584 adjuvanted with CAF01 + R848 induces antigen-specific antibodies but not T cell-based responses. (**A**) Schematic of i.m./i.m. immunization routes and schedule for CT584 with CAF01/R848. (**B**) Scatter plot showing CT584 specific IgG1 antibodies in mouse immune sera. The line indicates the median. *p*-values calculated using Welch's *t*-test. (**C**) Scatter plot showing CT584 specific IgG2a antibodies in mouse immune sera. The line indicates the median. *p*-values calculated using Welch's *t*-test. (**D**) Box and whiskers plot showing CD4 (**left**) and CD8 (**right**) expression in T cell populations from the draining lymph nodes of immunized mice. *p*-values calculated by Student's *t*-test. (**E**) Box and whiskers plot showing CD4 (**left**) and CD8 (**right**) expression in T cell populations from the spleen of immunized mice. *p*-values calculated by Student's *t*-test. (**F**) Scatter plot showing the percentage of draining lymph node immune cells expressing IFN-γ (**left**) and TNF-α (**right**) after ex vivo restimulation with antigen. The line indicates the median. *p*-values calculated by one-way ANOVA. (**G**) Scatter plot showing the percentage of splenocytes expressing IFN-γ (**left**) and TNF-α (**right**) after ex vivo restimulation with antigen. The line indicates the median. *p*-values calculated by one-way ANOVA. n.s. = not significant.

4. Discussion

There is a growing need for access to vaccines in the world, especially against *Ct*, where currently antibiotics are the only treatment modality. Although it is the most prevalent bacterial STI, its health consequences disproportionately impact poor and rural regions worldwide, where myriad logistical challenges towards detection and administration of aid remain [52]. Synthetic biology techniques such as CFPS can potentially address these

gaps, promising the ability to rapidly produce recombinant protein vaccine candidates and therapeutics at the point of use. CFPS lysates are amenable towards lyophilization and reconstitution in a just-add-water system, removing the necessity of cold-chain storage, making them ideal for low-cost low requirement solutions. Unlike recombinant single proteins, lyophilized cell-free systems are flexible and can rapidly produce potentially any target protein after reconstitution, as long as the correct DNA template is supplied. Advances in lyophilization techniques have enabled CFPS lysates to retain sufficient activity, even after weeks of storage at elevated temperatures, to produce active therapeutic enzymes such as crisantaspase, as well as immunogenic doses of a conjugate vaccine against enterotoxigenic *E. coli*. [53,54]. Demonstrably, pilot studies generating an on-demand vaccine against *Francisella tularensis* that is protective against lethal *F. tularensis* challenge in mice have also been performed [55].

Due to the inherent flexibility of CFPS systems, it is also possible to produce and solubilize even challenging chlamydial antigens, such as the integral membrane protein MOMP, for immunization studies [42,56]. Although bacterially derived recombinant MOMP and purified EBs performed the best overall in those studies, CFPS-produced MOMP was able to generate both humoral and cytokine responses and measurable protection in mice against respiratory challenge, with the added benefit of faster and easier production. Taking advantage of this flexibility, we used CFPS to produce and characterize the effects of a T3SS protein on protection against *Cm* infection.

T3SS function is highly conserved across chlamydial species and is required for infection [57], making it an attractive target for potential vaccines against *Ct*. While chlamydial gene expression can vary over the course of infection due to its distinctive bi-phasic life cycle, the T3SS is present in both EBs and RBs [12], suggesting a potential vaccine against T3SS components could be useful at all stages of infection. T3SS needle tip antigens from other organisms, such as *Y. pestis* [58,59] and *Salmonella enterica* [60,61], have been successfully used as vaccine antigens to protect against lethal challenge in mice and non-human primate models. Because CT584 was identified as a putative needle-tip protein in the chlamydial T3SS, we reasoned that it could be a suitable vaccine antigen candidate.

We produced and purified recombinant CT584 using CFPS and evaluated it for usage as a protective chlamydial vaccine antigen. We confirmed that CFPS-produced CT584 resembles its known structure (PDB: 4MLK [45]) using AFM data and simulations. In our mixed i.n./i.m. CT584 immunization regime, we observed an increase in IgG2a over IgG1 production, suggesting a skewing towards Th1-biased immune responses. As Th1 responses are important for protection against intracellular pathogens like chlamydia [46,62], it was an encouraging result. However, we did not see any protection from mice immunized with 20 μg of CT584, neither through i.m. nor i.n. routes, after i.n. challenge with *Cm* EBs. The CT584 immunized mice showed no differences from the PBS control, resulting in significant weight loss, increased lung weights indicative of ongoing inflammation, and increased lung IFUs. Interestingly, although we saw some measure of protection when combining 10 μg CT584 with 10 μg rMOMP, the effect was not better than rMOMP alone, suggesting that there were no synergistic effects and that the protection was likely driven by the addition of rMOMP.

CT584 has been incorporated into a few potential chlamydial vaccine formulations to date. As a recombinant protein fusion with other T3SS proteins, CopB and CopD, CT584 elicited a reduction in bacterial shedding after i.n./i.n. immunization in both *Cm* and *Ct* genital tract challenge models [16,17]. However, when using peptides designed from B-cell specific epitopes conjugated to a bacteriophage Qβ-based virus-like-particle (VLP) platform [63] through i.m. immunization, results were more mixed. Although initial experiments showed a reduction in *Ct* burden upon transcervical challenge, repeated experiments did not reach statistical significance. More recently, *Cm* CT584 (TC0873) was used for i.m./i.m./i.m. vaccination in mice but also failed to protect against *Cm* genital challenge, giving similar bacterial load and pathology to the PBS and mock controls [64].

Crucially, the two groups to have used full-length CT584 in their vaccine formulations obtained conflicting results: BD584 generated some partial protection as a vaccine candidate against *Cm* genital challenge in mice, while TC0873 did not. Since *Cm* TC0873 and *Ct* CT584 are nearly identical, it is unlikely to be due to differences in protein sequence or structure between the two antigens. There was a difference in the route of immunization between the two studies, with BD584 being administered mucosally; however, our results would suggest that both i.n. and i.m. routes are equally ineffective for CT584 alone. Thus, we can infer from this evidence that the success seen in BD584 is likely due to the partial CopB and CopD sequences in the fusion.

Additionally, it is important to point out that in the current study as well as the fusion protein and peptide studies described above, vaccination elicited robust antigen-specific antibody titers. While it is widely accepted that an effective chlamydia vaccine requires the induction of a cell-mediated immune response, the contribution of humoral immunity is less clear [65,66]. Pre-incubation of chlamydial EBs with immune sera from VLP-CT584 immunized mice from Webster et al. [63] before transplantation into naïve mice resulted in a significant reduction in upper genital tract bacterial burden compared to sera from VLP alone, highlighting the potential role antibodies may play in protection against chlamydial infection. However, it is important to note that while antibodies have been shown to reduce bacterial burden, especially upon reinfections in mouse models [67], the same phenomenon may not hold in human cohorts where antibody production for the prevention of pathology is a more complex interaction [68].

This, however, begs the following question: Since pre-opsonized EBs showed a marked reduction in bacterial load in mice and, presumably, infection efficiency, why are the antibodies generated against CT584 generally insufficient for protection against challenge with live EBs? Speculatively, it is possible that these antibodies merely recognize CT584 but are not neutralizing. Another possibility is that they are not present in sufficient titers on the mucosal surfaces—indeed, we observe significantly less IgG present in the vaginal washes compared to sera, as well as negligible IgA production, in our experiments. Although we used a respiratory challenge model, the reduced antibody titers on the mucosal surfaces would naturally preclude their effectiveness regardless of their neutralizing ability. Alternatively, there may be issues with CT584 antigen presentation in vivo. While CT584 immune sera could detect CT584 protein in EB lysates or purified samples through WB, the converse was not true. EB immune sera could not detect CT584 in any condition, suggesting that CT584 antigen in EBs may not be as immunogenic as the recombinant CT584 or that the antibodies generated against it only recognize a conformational epitope not detectable through WB. Irrespective of the cause, our data suggest that CFPS-produced CT584, alone or in combination with MOMP, may not be suitable as a vaccine candidate.

Although CT584 by itself did not elicit a protective immune response against *Cm* respiratory challenge in our formulations, other proteins of the T3SS may still present promising targets. T3SS function is crucial for chlamydial infection, and immunization using fusions of the terminal translocon pore proteins CopB and CopD showed encouraging results in both *Cm* and *Ct* mouse models [16,17]. Because fusion proteins, especially those of integral membrane proteins, may not be in the properly folded state, it may be possible to improve upon that antigen. Combining CFPS with nanodisc [56] technology would allow for the de novo synthesis of intact CopB and CopD pore complexes in membrane discs, mimicking their native structure, and could present a stronger immunogenic T3SS vaccine candidate for future studies.

5. Conclusions

We have demonstrated that CFPS-produced full-length *Ct* CT584 is not a protective vaccine antigen when adjuvanted with CpG-1826 + Montanide ISA 720, either alone or in combination with rMOMP, against respiratory chlamydial challenge in mice. Immunization through both i.n. or i.m. routes with CT584 generated systemic humoral (IgG) immune responses but negligible mucosal IgA production. Importantly, we saw no difference when

comparing CT584 to PBS control groups in terms of weight loss, lung inflammation, and bacterial load after challenge. Although CT584 is not effective as a vaccine antigen in our mouse model, CFPS approaches are flexible and can enable the rapid production and screening of other chlamydial antigens of interest.

Supplementary Materials: The following supporting information can be downloaded at https://www.mdpi.com/article/10.3390/vaccines12101134/s1, Figure S1: *Cm* TC0873 and *Ct* CT584 are nearly identical; Figure S2: *E. coli* DNA codon optimization for *Ct ct584*. Figure S3: Gating strategy for T cell populations and Th1 cytokines.

Author Contributions: Conceptualization, S.H.-P., L.M.d.l.M. and M.A.C.; Formal Analysis, S.H.-P., S.P., A.S., A.A.-O., F.A.B., M.L.S. and Y.Z.; Investigation, S.H.-P., S.P., A.S., A.A.-O., Y.Z., S.F.G., M.V.M., A.R. and L.M.d.l.M.; Writing—Original Draft Preparation, S.H.-P. and M.A.C.; Writing—Review and Editing, S.H.-P., S.P., A.S., A.A.-O., Y.Z., A.N., A.R., L.M.d.l.M. and M.A.C.; Visualization, S.H.-P., S.P. and A.S.; Supervision, A.N., A.R., L.M.d.l.M. and M.A.C.; Funding Acquisition, A.R., L.M.d.l.M. and M.A.C. All authors have read and agreed to the published version of the manuscript.

Funding: This research was funded by the National Institutes of Health, grant number U19 AI144184.

Institutional Review Board Statement: The animal study protocol was approved by the Institutional Review Board of the University of California, Irvine, the Institutional Animal Care and Use Committee (IACUC, AUP-23-049 (7/12/2023-7/12/2026), and the Lawrence Livermore National Laboratory IACUC (22-06-046 (6/17/2024-6/22/2025)).

Data Availability Statement: Data are contained within the article or Supplementary Materials.

Acknowledgments: We would like to thank D. Weilhammer for her help with animal and immunology studies. We would also like to thank P. D'haeseleer and L. Beckett for their helpful discussions and comments. Work at the Lawrence Livermore National Laboratory was performed under the auspices of the U.S. Department of Energy under Contract DE-AC52-07NA27344.

Conflicts of Interest: The authors declare no conflicts of interest.

References

1. Newman, L.; Rowley, J.; Vander Hoorn, S.; Wijesooriya, N.S.; Unemo, M.; Low, N.; Stevens, G.; Gottlieb, S.; Kiarie, J.; Temmerman, M. Global Estimates of the Prevalence and Incidence of Four Curable Sexually Transmitted Infections in 2012 Based on Systematic Review and Global Reporting. *PLoS ONE* **2015**, *10*, e0143304. [CrossRef] [PubMed]
2. den Heijer, C.D.J.; Hoebe, C.J.P.A.; Driessen, J.H.M.; Wolffs, P.; van den Broek, I.V.F.; Hoenderboom, B.M.; Williams, R.; de Vries, F.; Dukers-Muijrers, N.H.T.M. *Chlamydia trachomatis* and the Risk of Pelvic Inflammatory Disease, Ectopic Pregnancy, and Female Infertility: A Retrospective Cohort Study Among Primary Care Patients. *Clin. Infect. Dis.* **2019**, *69*, 1517–1525. [CrossRef] [PubMed]
3. Tang, W.; Mao, J.; Li, K.T.; Walker, J.S.; Chou, R.; Fu, R.; Chen, W.; Darville, T.; Klausner, J.D.; Tucker, J.D. Pregnancy and fertility-related adverse outcomes associated with *Chlamydia trachomatis* infection: A global systematic review and meta-analysis. *Sex. Transm. Infect.* **2020**, *96*, 322–329. [CrossRef] [PubMed]
4. Du, M.; Yan, W.; Jing, W.; Qin, C.; Liu, Q.; Liu, M.; Liu, J. Increasing incidence rates of sexually transmitted infections from 2010 to 2019: An analysis of temporal trends by geographical regions and age groups from the 2019 Global Burden of Disease Study. *BMC Infect. Dis.* **2022**, *22*, 574. [CrossRef] [PubMed]
5. Pinto, C.N.; Niles, J.K.; Kaufman, H.W.; Marlowe, E.M.; Alagia, D.P.; Chi, G.; Van Der Pol, B. Impact of the COVID-19 Pandemic on Chlamydia and Gonorrhea Screening in the U.S. *Am. J. Prev. Med.* **2021**, *61*, 386–393. [CrossRef]
6. Peterson, E.M.; You, J.Z.; Motin, V.; de la Maza, L.M. Intranasal immunization with *Chlamydia trachomatis*, serovar E, protects from a subsequent vaginal challenge with the homologous serovar. *Vaccine* **1999**, *17*, 2901–2907. [CrossRef]
7. Sowa, S.; Sowa, J.; Collier, L.H.; Blyth, W.A. Trachoma vaccine field trials in The Gambia. *J. Hyg. (Lond)* **1969**, *67*, 699–717. [CrossRef]
8. Woolridge, R.L.; Grayston, J.T.; Chang, I.H.; Cheng, K.H.; Yang, C.Y.; Neave, C. Field trial of a monovalent and of a bivalent mineral oil adjuvant trachoma vaccine in Taiwan school children. *Am. J. Ophthalmol.* **1967**, *63*, 1645–1650. [CrossRef]
9. Caldwell, H.D.; Kromhout, J.; Schachter, J. Purification and partial characterization of the major outer membrane protein of *Chlamydia trachomatis*. *Infect. Immun.* **1981**, *31*, 1161–1176. [CrossRef]
10. de la Maza, L.M.; Darville, T.L.; Pal, S. *Chlamydia trachomatis* vaccines for genital infections: Where are we and how far is there to go? *Expert. Rev. Vaccines* **2021**, *20*, 421–435. [CrossRef]
11. Nans, A.; Kudryashev, M.; Saibil, H.R.; Hayward, R.D. Structure of a bacterial type III secretion system in contact with a host membrane in situ. *Nat. Commun.* **2015**, *6*, 10114. [CrossRef] [PubMed]

12. Shaw, E.I.; Dooley, C.A.; Fischer, E.R.; Scidmore, M.A.; Fields, K.A.; Hackstadt, T. Three temporal classes of gene expression during the *Chlamydia trachomatis* developmental cycle. *Mol. Microbiol.* **2000**, *37*, 913–925. [CrossRef] [PubMed]
13. Bailey, L.; Gylfe, A.; Sundin, C.; Muschiol, S.; Elofsson, M.; Nordstrom, P.; Henriques-Normark, B.; Lugert, R.; Waldenstrom, A.; Wolf-Watz, H.; et al. Small molecule inhibitors of type III secretion in Yersinia block the *Chlamydia pneumoniae* infection cycle. *FEBS Lett.* **2007**, *581*, 587–595. [CrossRef] [PubMed]
14. Muschiol, S.; Bailey, L.; Gylfe, A.; Sundin, C.; Hultenby, K.; Bergstrom, S.; Elofsson, M.; Wolf-Watz, H.; Normark, S.; Henriques-Normark, B. A small-molecule inhibitor of type III secretion inhibits different stages of the infectious cycle of *Chlamydia trachomatis*. *Proc. Natl. Acad. Sci. USA* **2006**, *103*, 14566–14571. [CrossRef] [PubMed]
15. Muschiol, S.; Normark, S.; Henriques-Normark, B.; Subtil, A. Small molecule inhibitors of the Yersinia type III secretion system impair the development of Chlamydia after entry into host cells. *BMC Microbiol.* **2009**, *9*, 75. [CrossRef]
16. Bulir, D.C.; Liang, S.; Lee, A.; Chong, S.; Simms, E.; Stone, C.; Kaushic, C.; Ashkar, A.; Mahony, J.B. Immunization with chlamydial type III secretion antigens reduces vaginal shedding and prevents fallopian tube pathology following live *C. muridarum* challenge. *Vaccine* **2016**, *34*, 3979–3985. [CrossRef]
17. Liang, S.; Mahony, J.B. Intranasal vaccination with a Chimeric Chlamydial Antigen BD584 confers protection against *Chlamydia trachomatis* genital tract infection. *J. Vaccines Immunol.* **2020**, *6*, 010–017. [CrossRef]
18. Bulir, D.C.; Waltho, D.A.; Stone, C.B.; Liang, S.; Chiang, C.K.; Mwawasi, K.A.; Nelson, J.C.; Zhang, S.W.; Mihalco, S.P.; Scinocca, Z.C.; et al. Chlamydia Outer Protein (Cop) B from *Chlamydia pneumoniae* possesses characteristic features of a type III secretion (T3S) translocator protein. *BMC Microbiol.* **2015**, *15*, 163. [CrossRef]
19. Bulir, D.C.; Waltho, D.A.; Stone, C.B.; Mwawasi, K.A.; Nelson, J.C.; Mahony, J.B. *Chlamydia pneumoniae* CopD translocator protein plays a critical role in type III secretion (T3S) and infection. *PLoS ONE* **2014**, *9*, e99315. [CrossRef]
20. Markham, A.P.; Jaafar, Z.A.; Kemege, K.E.; Middaugh, C.R.; Hefty, P.S. Biophysical characterization of *Chlamydia trachomatis* CT584 supports its potential role as a type III secretion needle tip protein. *Biochemistry* **2009**, *48*, 10353–10361. [CrossRef]
21. Hufnagel, K.; Hoenderboom, B.; Harmel, C.; Rohland, J.K.; van Benthem, B.H.B.; Morre, S.A.; Waterboer, T. *Chlamydia trachomatis* Whole-Proteome Microarray Analysis of The Netherlands Chlamydia Cohort Study. *Microorganisms* **2019**, *7*, 703. [CrossRef] [PubMed]
22. Cowan, C.; Philipovskiy, A.V.; Wulff-Strobel, C.R.; Ye, Z.; Straley, S.C. Anti-LcrV antibody inhibits delivery of Yops by Yersinia pestis KIM5 by directly promoting phagocytosis. *Infect. Immun.* **2005**, *73*, 6127–6137. [CrossRef] [PubMed]
23. Philipovskiy, A.V.; Cowan, C.; Wulff-Strobel, C.R.; Burnett, S.H.; Kerschen, E.J.; Cohen, D.A.; Kaplan, A.M.; Straley, S.C. Antibody against V antigen prevents Yop-dependent growth of Yersinia pestis. *Infect. Immun.* **2005**, *73*, 1532–1542. [CrossRef] [PubMed]
24. de la Maza, L.M.; Pal, S.; Khamesipour, A.; Peterson, E.M. Intravaginal Inoculation of Mice with the *Chlamydia trachomatis* Mouse Pneumonitis Biovar Results in Infertility. *Infect. Immun.* **1994**, *62*, 2094–2097. [CrossRef] [PubMed]
25. Nigg, C. An unidentified virus which produces pneumonia and systemic infection in mice. *Science* **1942**, *995*, 49–50. [CrossRef]
26. Garenne, D.; Haines, M.C.; Romantseva, E.F.; Freemont, P.; Strychalski, E.A.; Noireaux, V. Cell-free gene expression. *Nat. Rev. Methods Primers* **2021**, *1*, 49. [CrossRef]
27. Batista, A.C.; Soudier, P.; Kushwaha, M.; Faulon, J.L. Optimising protein synthesis in cell-free systems, a review. *Eng. Biol.* **2021**, *5*, 10–19. [CrossRef]
28. Li, X.; Abrahams, C.L.; Yu, A.; Embry, M.; Henningsen, R.; DeAlmeida, V.I.; Matheny, S.; Kline, T.; Yam, A.Y.; Stafford, R.L.; et al. Targeting CD74 in B-cell non-Hodgkin lymphoma with the antibody-drug conjugate STRO-001. *Oncotarget* **2023**, *14*, 1–13. [CrossRef]
29. Li, X.; Zhou, S.; Abrahams, C.L.; Krimm, S.; Smith, J.; Bajjuri, K.; Stephenson, H.T.; Henningsen, R.; Hanson, J.; Heibeck, T.H.; et al. Discovery of STRO-002, a Novel Homogeneous ADC Targeting Folate Receptor Alpha, for the Treatment of Ovarian and Endometrial Cancers. *Mol. Cancer Ther.* **2023**, *22*, 155–167. [CrossRef]
30. Fairman, J.; Agarwal, P.; Barbanel, S.; Behrens, C.; Berges, A.; Burky, J.; Davey, P.; Fernsten, P.; Grainger, C.; Guo, S.; et al. Non-clinical immunological comparison of a Next-Generation 24-valent pneumococcal conjugate vaccine (VAX-24) using site-specific carrier protein conjugation to the current standard of care (PCV13 and PPV23). *Vaccine* **2021**, *39*, 3197–3206. [CrossRef]
31. Putman, T.; Hybiske, K.; Jow, D.; Afrasiabi, C.; Lelong, S.; Cano, M.A.; Wu, C.; Su, A.I. ChlamBase: A curated model organism database for the Chlamydia research community. *Database* **2019**, *2019*, baz041. [CrossRef] [PubMed]
32. Pal, S.; Peterson, E.M.; de la Maza, L.M. Vaccination with the *Chlamydia trachomatis* major outer membrane protein can elicit an immune response as protective as that resulting from inoculation with live bacteria. *Infect. Immun.* **2005**, *73*, 8153–8160. [CrossRef] [PubMed]
33. Sun, G.; Pal, S.; Weiland, J.; Peterson, E.M.; de la Maza, L.M. Protection against an intranasal challenge by vaccines formulated with native and recombinant preparations of the *Chlamydia trachomatis* major outer membrane protein. *Vaccine* **2009**, *27*, 5020–5025. [CrossRef] [PubMed]
34. Kodera, N.; Sakashita, M.; Ando, T. Dynamic proportional-integral-differential controller for high-speed atomic force microscopy. *Rev. Sci. Instrum.* **2006**, *77*, 083704. [CrossRef]
35. Uchihashi, T.; Kodera, N.; Ando, T. Guide to video recording of structure dynamics and dynamic processes of proteins by high-speed atomic force microscopy. *Nat. Protoc.* **2012**, *7*, 1193–1206. [CrossRef] [PubMed]
36. Zhang, Y.; Tunuguntla, R.H.; Choi, P.O.; Noy, A. Real-time dynamics of carbon nanotube porins in supported lipid membranes visualized by high-speed atomic force microscopy. *Philos. Trans. R. Soc. B Biol. Sci.* **2017**, *372*, 20160226. [CrossRef]

37. Niina, T.; Matsunaga, Y.; Takada, S. Rigid-body fitting to atomic force microscopy images for inferring probe shape and biomolecular structure. *PLoS Comput. Biol.* **2021**, *17*, e1009215. [CrossRef]
38. Nečas, D.; Klapetek, P. Gwyddion: An open-source software for SPM data analysis. *Open Phys.* **2012**, *10*, 181–188. [CrossRef]
39. Agger, E.M.; Rosenkrands, I.; Hansen, J.; Brahimi, K.; Vandahl, B.S.; Aagaard, C.; Werninghaus, K.; Kirschning, C.; Lang, R.; Christensen, D.; et al. Cationic liposomes formulated with synthetic mycobacterial cordfactor (CAF01): A versatile adjuvant for vaccines with different immunological requirements. *PLoS ONE* **2008**, *3*, e3116. [CrossRef]
40. Pal, S.; Tifrea, D.F.; Follmann, F.; Andersen, P.; de la Maza, L.M. The cationic liposomal adjuvants CAF01 and CAF09 formulated with the major outer membrane protein elicit robust protection in mice against a *Chlamydia muridarum* respiratory challenge. *Vaccine* **2017**, *35*, 1705–1711. [CrossRef]
41. Pal, S.; Fielder, T.J.; Peterson, E.M.; de la Maza, L.M. Protection against infertility in a BALB/c mouse salpingitis model by intranasal immunization with the mouse pneumonitis biovar of *Chlamydia trachomatis*. *Infect. Immun.* **1994**, *62*, 3354–3362. [CrossRef] [PubMed]
42. Tifrea, D.F.; He, W.; Pal, S.; Evans, A.C.; Gilmore, S.F.; Fischer, N.O.; Rasley, A.; Coleman, M.A.; de la Maza, L.M. Induction of Protection in Mice against a *Chlamydia muridarum* Respiratory Challenge by a Vaccine Formulated with the Major Outer Membrane Protein in Nanolipoprotein Particles. *Vaccines* **2021**, *9*, 755. [CrossRef] [PubMed]
43. Tuller, T.; Waldman, Y.Y.; Kupiec, M.; Ruppin, E. Translation efficiency is determined by both codon bias and folding energy. *Proc. Natl. Acad. Sci. USA* **2010**, *107*, 3645–3650. [CrossRef] [PubMed]
44. Bolanos-Garcia, V.M.; Davies, O.R. Structural analysis and classification of native proteins from *E. coli* commonly co-purified by immobilised metal affinity chromatography. *Biochim. Biophys. Acta* **2006**, *1760*, 1304–1313. [CrossRef]
45. Barta, M.L.; Hickey, J.; Kemege, K.E.; Lovell, S.; Battaile, K.P.; Hefty, P.S. Structure of CT584 from *Chlamydia trachomatis* refined to 3.05 A resolution. *Acta Crystallogr. Sect. F Struct. Biol. Cryst. Commun.* **2013**, *69*, 1196–1201. [CrossRef]
46. Pal, S.; Cruz-Fisher, M.I.; Cheng, C.; Carmichael, J.R.; Tifrea, D.F.; Tatarenkova, O.; de la Maza, L.M. Vaccination with the recombinant major outer membrane protein elicits long-term protection in mice against vaginal shedding and infertility following a *Chlamydia muridarum* genital challenge. *NPJ Vaccines* **2020**, *5*, 90. [CrossRef]
47. Chu, R.S.; Targoni, O.S.; Krieg, A.M.; Lehmann, P.V.; Harding, C.V. CpG Oligodeoxynucleotides Act as Adjuvants that Switch on T Helper 1 (Th1) Immunity. *J. Exp. Med.* **1997**, *186*, 1623–1631. [CrossRef]
48. Marques, R.F.; de Melo, F.M.; Novais, J.T.; Soares, I.S.; Bargieri, D.Y.; Gimenez, A.M. Immune System Modulation by the Adjuvants Poly (I:C) and Montanide ISA 720. *Front. Immunol.* **2022**, *13*, 910022. [CrossRef]
49. Pal, S.; Slepenkin, A.; Felgner, J.; Huw Davies, D.; Felgner, P.; de la Maza, L.M. Evaluation of Four Adjuvant Combinations, IVAX-1, IVAX-2, CpG-1826+Montanide ISA 720 VG and CpG-1018+Montanide ISA 720 VG, for Safety and for Their Ability to Elicit Protective Immune Responses in Mice against a Respiratory Challenge with *Chlamydia muridarum*. *Pathogens* **2023**, *12*, 863. [CrossRef]
50. Knudsen, N.P.; Olsen, A.; Buonsanti, C.; Follmann, F.; Zhang, Y.; Coler, R.N.; Fox, C.B.; Meinke, A.; D'Oro, U.; Casini, D.; et al. Different human vaccine adjuvants promote distinct antigen-independent immunological signatures tailored to different pathogens. *Sci. Rep.* **2016**, *6*, 19570. [CrossRef]
51. Vasilakos, J.P.; Smith, R.M.; Gibson, S.J.; Lindh, J.M.; Pederson, L.K.; Reiter, M.J.; Smith, M.H.; Tomai, M.A. Adjuvant activities of immune response modifier R-848: Comparison with CpG ODN. *Cell Immunol.* **2000**, *204*, 64–74. [CrossRef] [PubMed]
52. Unemo, M.; Bradshaw, C.S.; Hocking, J.S.; de Vries, H.J.C.; Francis, S.C.; Mabey, D.; Marrazzo, J.M.; Sonder, G.J.B.; Schwebke, J.R.; Hoornenborg, E.; et al. Sexually transmitted infections: Challenges ahead. *Lancet Infect. Dis.* **2017**, *17*, e235–e279. [CrossRef] [PubMed]
53. Warfel, K.F.; Williams, A.; Wong, D.A.; Sobol, S.E.; Desai, P.; Li, J.; Chang, Y.F.; DeLisa, M.P.; Karim, A.S.; Jewett, M.C. A Low-Cost, Thermostable, Cell-Free Protein Synthesis Platform for On-Demand Production of Conjugate Vaccines. *ACS Synth. Biol.* **2023**, *12*, 95–107. [CrossRef] [PubMed]
54. Wilding, K.M.; Zhao, E.L.; Earl, C.C.; Bundy, B.C. Thermostable lyoprotectant-enhanced cell-free protein synthesis for on-demand endotoxin-free therapeutic production. *New Biotechnol.* **2019**, *53*, 73–80. [CrossRef]
55. Stark, J.C.; Jaroentomeechai, T.; Moeller, T.D.; Hershewe, J.M.; Warfel, K.F.; Moricz, B.S.; Martini, A.M.; Dubner, R.S.; Hsu, K.J.; Stevenson, T.C.; et al. On-demand biomanufacturing of protective conjugate vaccines. *Sci. Adv.* **2021**, *7*, eabe9444. [CrossRef] [PubMed]
56. He, W.; Felderman, M.; Evans, A.C.; Geng, J.; Homan, D.; Bourguet, F.; Fischer, N.O.; Li, Y.; Lam, K.S.; Noy, A.; et al. Cell-free production of a functional oligomeric form of a *Chlamydia* major outer-membrane protein (MOMP) for vaccine development. *J. Biol. Chem.* **2017**, *292*, 15121–15132. [CrossRef]
57. Mueller, K.E.; Plano, G.V.; Fields, K.A. New frontiers in type III secretion biology: The Chlamydia perspective. *Infect. Immun.* **2014**, *82*, 2–9. [CrossRef]
58. Fellows, P.; Price, J.; Martin, S.; Metcalfe, K.; Krile, R.; Barnewall, R.; Hart, M.K.; Lockman, H. Characterization of a Cynomolgus Macaque Model of Pneumonic Plague for Evaluation of Vaccine Efficacy. *Clin. Vaccine Immunol.* **2015**, *22*, 1070–1078. [CrossRef]
59. Heath, D.G.; Anderson, G.W., Jr.; Mauro, J.M.; Welkos, S.L.; Andrews, G.P.; Adomovicz, J.; Friedlander, A.M. Protection against experimental bubonic and pneumonic plague by a recombinant capsular Fl-V antigen fusion protein vaccine. *Vaccine* **1998**, *16*, 1131–1137. [CrossRef]

60. Jneid, B.; Moreau, K.; Plaisance, M.; Rouaix, A.; Dano, J.; Simon, S. Role of T3SS-1 SipD Protein in Protecting Mice against Non-typhoidal *Salmonella typhimurium*. *PLoS Neglected Trop. Dis.* **2016**, *10*, e0005207. [CrossRef]
61. Martinez-Becerra, F.J.; Kumar, P.; Vishwakarma, V.; Kim, J.H.; Arizmendi, O.; Middaugh, C.R.; Picking, W.D.; Picking, W.L. Characterization and Protective Efficacy of Type III Secretion Proteins as a Broadly Protective Subunit Vaccine against *Salmonella enterica* Serotypes. *Infect. Immun.* **2018**, *86*, e00473-17. [CrossRef] [PubMed]
62. Stary, G.; Olive, A.; Radovic-Moreno, A.F.; Gondek, D.; Alvarez, D.; Basto, P.A.; Perro, M.; Vrbanac, V.D.; Tager, A.M.; Shi, J.; et al. A mucosal vaccine against *Chlamydia trachomatis* generates two waves of protective memory T cells. *Science* **2015**, *348*, aaa8205. [CrossRef] [PubMed]
63. Webster, E.; Seiger, K.W.; Core, S.B.; Collar, A.L.; Knapp-Broas, H.; Graham, J.; Shrestha, M.; Afzaal, S.; Geisler, W.M.; Wheeler, C.M.; et al. Immunogenicity and Protective Capacity of a Virus-like Particle Vaccine against *Chlamydia trachomatis* Type 3 Secretion System Tip Protein, CT584. *Vaccines* **2022**, *10*, 111. [CrossRef] [PubMed]
64. Lu, C.; Wang, J.; Zhong, G. Preclinical screen for protection efficacy of chlamydial antigens that are immunogenic in humans. *Infect. Immun.* **2023**, *91*, e0034923. [CrossRef]
65. Ramsey, K.H.; Soderberg, L.S.; Rank, R.G. Resolution of chlamydial genital infection in B-cell-deficient mice and immunity to reinfection. *Infect. Immun.* **1988**, *56*, 1320–1325. [CrossRef]
66. Williams, D.M.; Grubbs, B.; Schachter, J. Primary murine *Chlamydia trachomatis* pneumonia in B-cell-deficient mice. *Infect. Immun.* **1987**, *55*, 2387–2390. [CrossRef]
67. Morrison, S.G.; Morrison, R.P. A predominant role for antibody in acquired immunity to chlamydial genital tract reinfection. *J. Immunol.* **2005**, *175*, 7536–7542. [CrossRef]
68. Liu, C.; Hufnagel, K.; O'Connell, C.M.; Goonetilleke, N.; Mokashi, N.; Waterboer, T.; Tollison, T.S.; Peng, X.; Wiesenfeld, H.C.; Hillier, S.L.; et al. Reduced Endometrial Ascension and Enhanced Reinfection Associated With Immunoglobulin G Antibodies to Specific *Chlamydia trachomatis* Proteins in Women at Risk for Chlamydia. *J. Infect. Dis.* **2022**, *225*, 846–855. [CrossRef]